Supramolecular Peptide Depots for Glucose-Responsive Glucagon Delivery

Weike Chen,[1] Sihan Yu,[1] Bernice Webber,[1] Emily L. DeWolf,[1] Rory Kilmer,[1] Sijie Xian,[1] Connor R. Schmidt,[1] Elizabeth M. Power,[1] Matthew J. Webber[1,*]

1- University of Notre Dame, Department of Chemical & Biomolecular Engineering, Notre Dame, IN 46556 USA

*- Correspondences addressed to: mwebber@nd.edu

Abstract: This study investigates the development of a supramolecular peptide amphiphile (PA) material functionalized with phenylboronic acid (PBA) for glucose-responsive glucagon delivery. The PA-PBA system self-assembles into nanofibrillar hydrogels in the presence of physiological glucose levels, resulting in stable hydrogels capable of releasing glucagon under hypoglycemic conditions. Glucose responsiveness is driven by reversible binding between PBA and glucose, which modulates the electrostatic interactions necessary for hydrogel formation and dissolution. Through comprehensive *in vitro* characterization, including circular dichroism, zeta potential measurements, and rheological assessments, the PA-PBA system is found to exhibit glucose-dependent assembly, enabling controlled glucagon release that is inversely related to glucose concentration. Glucagon release is accelerated under low glucose conditions, simulating a hypoglycemic state, with a reduced rate seen at higher glucose levels. Evaluation of the platform *in vivo* using a type 1 diabetic mouse model demonstrates efficacy in protecting against insulin-induced hypoglycemia by restoring blood glucose levels following an insulin overdose. The ability to tailor glucagon release in response to fluctuating glucose concentrations underscores the potential of this platform for improving glycemic control. These findings suggest that glucose-stabilized supramolecular peptide hydrogels hold significant promise for responsive drug delivery applications, offering an approach to manage glucose levels in diabetes and other metabolic disorders.

Keywords: Drug Delivery; Materials Chemistry; Hydrogels; Self-Assembly

1. Introduction

Living organisms respond to a variety of internal or external stimuli, sensing changes in their environment and responding through an assortment of biological functions. Blood glucose homeostasis, a control network driven by the complex signaling of a number of hormones and incretins and regulated by the central nervous system,[(1)–(4)] is one such process. Toward the creation of more life-like properties, synthetic biomaterials have been similarly designed to achieve stimuli-responsive functionality and, in so doing, better interface with physiological systems.[(5)–(7)] Engineering glucose-responsive biomaterials is a particularly active area of research,[(8)–(11)] owing in large part to the dramatic increase in prevalence of diabetes in recent years.[(12)] These systems aim to restore blood glucose homeostasis, which is dysregulated as part of the pathophysiology of diabetes, through controlled and on-demand release of key hormones like insulin and, in a less explored direction, glucagon.

The emergence of supramolecular materials, prepared *via* specific and ordered non-covalent molecular recognition motifs, offers a useful design approach in the preparation of biomaterials and technologies for drug delivery.[(13),(14)] The underlying dynamic molecular-scale interactions give rise to advantageous bulk dynamic properties, including shear-thinning and self-healing for facile injection-centered administration.[(15)] Moreover, the non-covalent constitution of these materials makes them especially susceptible to changes in their environment, regulating the extent and magnitude of their cohesive interactions and offering opportunities for design of stimuli-responsive biomaterials.[(16),(17)] The creation of supramolecular polymers *via* peptide self-assembly yields a specific class of supramolecular biomaterials consisting of bio-inspired nanofibrillar structures and hydrogel networks that have empowered a number of applications as biomaterials and in drug delivery.[(18)–(21)] Peptides offer particularly useful building blocks for the construction of supramolecular biomaterials due to their chemical versatility, biocompatibility, and biodegradability.[(22)] By precisely tailoring molecular features used in self-assembly,[(23)] peptide-based supramolecular biomaterials have thus been designed with dynamic behaviors that respond to disease-specific stimuli such as pH,[(24)] enzymes,[(25)] and redox conditions.[(26)]

Toward applications in blood glucose control, glucose-responsive supramolecular biomaterials prepared from peptide self-assembly have also been explored. The local microenvironmental acidification arising from catalytic conversion of glucose to gluconic acid by the glucose oxidase (GOx) enzyme has been used alongside cationic peptide assemblies for glucose-responsive materials that

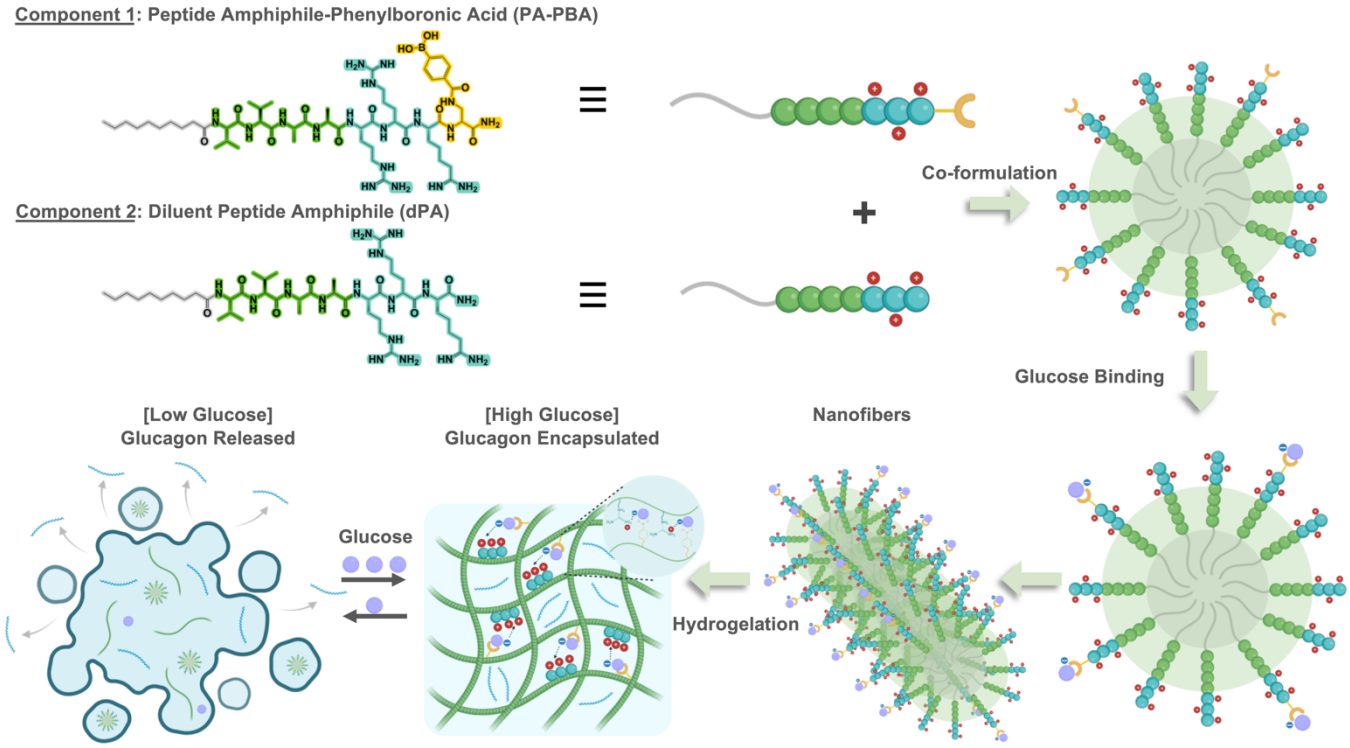

Figure 1. Cartoon schematic illustrating the glucose-responsive supramolecular peptide depots for on-demand glucagon release. A peptide amphiphile (PA) was endowed with a glucose-binding phenylboronic acid (PBA) molecule (PA-PBA). To facilitate nanofiber formation and hydrogelation, a diluent peptide amphiphile (dPA) was synthesized and co-formulated with PA-PBA. When binding with glucose, these mixtures undergo a nanostructure transformation from micelles to elongated nanofibers, enabling the formation of injectable hydrogels. At low glucose conditions, the dissociation of the PBA-glucose complex allows hydrogels swell and release glucagon.

deliver insulin *via* glucose-directed disassembly.[27],[28] More recent efforts have sought to use glucose as a stabilizing cue in the design of peptide self-assemblies, with the goal of releasing glucagon under conditions of a low glucose stimulus to correct for hypoglycemic (low blood glucose) conditions. This has been achieved through anionic peptide amphiphiles (PAs) in combination with GOx, wherein acidification in the presence of glucose drives self-assembly and hydrogelation while the absence of glucose triggers disassembly and glucagon release.[29] More recent efforts have included glucose-binding phenylboronic acid (PBA) motifs on both oligopeptides and PAs for the same purpose of preparing glucose-stabilized materials.[30],[31] PBAs are Lewis acids that bind reversibly to *cis*-1,2 diols like glucose, stabilizing the anionic tetrahedral boronate species.[9] Accordingly, inclusion of PBAs on self-assembling peptides enables tunable electrostatic interactions to modulate supramolecular cohesion and regulate self-assembly.

Herein, a PA bearing a terminal PBA motif (PA-PBA) is reported that, upon mixing with a diluent PA (dPA) in the presence of glucose, can form self-assembled nanofibers that further elongate and entangle to form self-supporting hydrogels (***Fig 1***). Glucose is essential for high aspect-ratio nanofiber formation and hydrogelation, and in the absence of glucose smaller nanostructures arise that do not form hydrogels. Accordingly, hydrogels formed from these materials in the presence of glucose can become destabilized under low glucose conditions to release encapsulated glucagon. In an animal model of insulin overdose and hypoglycemia, the administration of the PA-PBA/dPA hydrogels offers some protection and improved blood glucose recovery.

2. Experimental Methods

2.1 Peptide Synthesis & Purification. Peptides were synthesized by solid-phase Fmoc synthesis procedures using a CEM Liberty Blue microwave synthesizer. Fmoc groups on Rink amide resin (0.72 mmeq/g, 100-200 mesh) were removed by 20% (v/v) piperidine in *N,N*-dimethylformamide (DMF), followed by a coupling reaction with diisopropylcarbodiimide (DIC) and Oxyma in DMF under microwave heating. For C_{10}-$V_2A_2R_3$-Dap(Mtt) peptide, removal of a selectively labile Mtt protecting group was performed using 5% TFA in dichloromethane (DCM), followed by conjugation of 4-carboxyphenylboronic acid to the free amine on the side chain of Dap residue. After completion of synthesis, peptides were cleaved from resin using a mixture of trifluoroacetic acid (TFA), triisopropanolsilane (TIS), and H_2O (95:2.5:2.5, v/v/v) for 3 h at room temperature. The resin was washed with DCM and the mixture of TFA and DCM was concentrated under vacuum to remove most solvent. The residual peptide solution was precipitated in cold diethyl ether, followed by centrifugation and diethyl ether washing and drying under vacuum overnight. The crude peptides were dissolved in

hexafluoro-2-propanol (HFIP) and purified on a Biotage Isolera using a reversed-phase bio-C_{18} flash cartridge (25 g) with a linear gradient of water to acetonitrile (ACN), each containing 0.1% TFA. The elution was monitored at 220 and 260 nm. The purity of collected fractions were verified by electrospray ionization mass spectrometry (ESI-MS, Advin) and high performance-liquid chromatography (HPLC) using a C_{18} Gemini (Phenomenex) column. Dasiglucagon and MCA-labeled dasiglucagon were synthesized and purified using similar methodology, according to methods previously described.[29]

2.2 Preparation of PA-PBA/dPA Hydrogels. PA-PBA and PA peptides were individually dissolved at 10 mg/mL in an ACN/H_2O (1:1 v/v) mixture and mixed at a mass fraction of PA-PBA to dPA of 10%, 20%, 30%, or 40%. The mixed samples were then frozen in liquid nitrogen and dried by lyophilization to remove all solvent. The co-formulated peptide powders were then dissolved in dI water at a concentration of 4% (w/v), and after solubilized were mixed with 2X HEPES buffer (pH 7.4, 10 mM) and diluted to a final a concentration of 2% (w/v) and glucose concentrations of 0, 25, 50, 100, or 200 mg/dL.

2.3 Circular Dichroism (CD) Spectroscopy. CD spectroscopy was performed on a Jasco 710 CD spectrometer. PA-PBA/dPA samples were mixed and prepared as above and diluted in HEPES buffer (pH 7.4, 10 mM) at various glucose concentrations (0, 25, 50, 100, or 200 mg/dL) to a concentration of 0.5% (w/v). The CD spectra were collected from 250 nm to 195 nm at room temperature using a 0.1 mm cuvette, a bandwidth at 0.1 nm, scan rate at 50 nm/min, and a response time of 2 s. The spectra of HEPES buffer (pH 7.4, 10 mM) was measured as background and subtracted from all samples. The raw data was converted to mean residue ellipticity (MRE) by using the formula θ=(1000*mDeg)/(c*n*l) where c is the peptide concentration in mM, (n) is the number of amino acids, and (l) is the pathlength of the cell used in the unit of millimeter.

2.4 Transmission Electron Microscopy (TEM). PA-PBA/dPA samples were prepared as above at 2% (w/v) in HEPES buffer with varying glucose levels. Immediately before preparing grids, samples were further diluted in the same HEPES buffer containing 0, 25, 50, 100, 200 mg/dL glucose to a final concentration of 0.1% (w/v). A 10 µL sample was pipetted onto a lacey carbon grid (Ted Pella 01824). After 2 min, the sample solution was removed by filter paper and 10 µL of 2% (w/v) uranyl acetate solution was pipetted onto the grid for negative staining. After 2 min, the excess uranyl acetate solution was removed by filter paper and grids were dried overnight before imaging on the Talos F200i (S)TEM 20-200 kV field emission (scanning) TEM.

2.5 Zeta Potential. PA-PBA/dPA samples were prepared as above in HEPES buffer (pH 7.4, 10 mM, 150 mM NaCl) at concentration of 0.5% (w/v) with addition of 0, 25, 50, 100, or 200 mg/dL glucose. The zeta potential was measured using a Malvern Zetasizer with a Huckel model at 25°C. The zeta potential measurements were collected in triplicate.

2.6 Rheological Characterization. PA-PBA/dPA samples were prepared as above in HEPES buffer (pH 7.4, 10 mM, 150 mM NaCl) at 2% (w/v) within addition of glucose concentrations of 0, 25, 50, 100, or 200 mg/dL and their rheological properties were evaluated using TA Instruments Discovery HR-2 rheometer. The linear viscoelastic range was determined by an amplitude sweep performed at 1 rad/s. A frequency sweep was then performed at constant strain of 0.5%. The gelation over time was evaluated via a time sweep at a constant 0.5% strain and 1 rad/s. Recovery following high strain for PA-PBA/dPA hydrogel at glucose 100 mg/dL was evaluated by a step-strain cycling between 0.5% strain for 2 min and 100% strain for 30 s at a constant angular frequency of 1 rad/s. The shear-thinning property of PA-PBA/PA hydrogel at glucose 100 mg/dL was studied under steady shear flow over a shear rate range from 0.001 to 88 s^{-1}.

2.7 Glucagon Release. PA-PBA/dPA hydrogels were prepared as above at 2% (w/v) in HEPES buffer at glucose concentration of 100 mg/dL and included 0.1 mg/mL MCA-dasiglucagon. MCA-dasiglucagon was synthesized as previously described.[29] Following preparation, 50 µL hydrogels were incubated within 12-well plates in 2 mL of bulk HEPES buffer containing 0, 25, 50, 100, or 200 mg/dL glucose. At each time point, a sample of half of the bulk buffer was removed and subjected to fluorescence analysis (*Ex: 324 nm, Em: 380 nm*) on a Tecan M200 plate reader. At each time point, after removing half of the volume of the bulk buffer (1 mL), fresh buffer of equal volume was added to simulate conditions of bulk dilution.

2.8 In Vivo Hypoglycemia Protection. Animal studies were performed in accordance with guidelines for the care and use of laboratory animals and protocols (#21-11-6916) were approved by the University of Notre Dame Institutional Animal Care and Use Committee (IACUC). A previously established hypoglycemic rescue model in mice was performed as described.[29] Male C57BL6/J mice (8 weeks) were administered streptozotocin (STZ) *i.p.* at a dose of 150 mg/kg to induce an insulin-deficient phenotype. After 10-12 d, non-fasting blood glucose levels reached 600+ mg/dL and the *in vivo* study was initiated. After 8 h fasting, mice with blood glucose levels (BGL) higher than 450 mg/dL were treated with 0.5 IU/kg basal *insulin detemir* via *s.c.* injection. Once the BGL was reduced to 180 mg/dL, mice were randomized into two groups (n=9) and treated with single *s.c.* injection of 0.1 mL PA-PBA/dPA hydrogel containing 5 µg dasiglucagon and compared to a single *s.c.* injection of 5 µg dasiglucagon. After 2 h, AOF recombinant human insulin was administered at a dose of 2.8 IU/kg via *i.p.* injection to induce severe hypoglycemia. BGL was measured by handheld blood glucose monitor throughout the study. Mice with "high" BGL readings were noted with a 600 mg/dL, while "low" BGL readings were noted with a 20 mg/dL and triaged from the study due to severe morbidity or mortality.

2.9 Statistical Analysis. Statistical analysis was performed on replicates from zeta potential studies and release studies using a one-way analysis of variance (ANOVA) with Tukey *post hoc* testing. Final blood glucose levels were compared

using Student's t-test. All statistics were performed using GraphPad Prism v10. Details about the sample number (n) and method of statistical testing can be found in the corresponding figure captions.

3. Results & Discussion

3.1 Molecular Design of Peptides. Peptide amphiphiles (PAs) are a versatile and well-studied platform for the preparation of hydrogel biomaterials.[32] The design of PA-PBA (C_{10}–$V_2A_2R_3$Dap(PBA), ***Fig 1***) was adopted from a prior report.[31] A saturated alkyl (C_{10}) tail providing a hydrophobic driving force for self-assembly in water was functionalized with two valine (V_2) and two alanine (A_2) residues to promote intermolecular parallel β-sheet structures, while three positively charged arginine (R_3) residues offered hydrophilic motifs to impart amphiphilicity. A diaminopropionic acid (Dap) was included at the C-terminus and coupled on-resin with 4-carboxyphenylboronic acid (PBA) *via* selective deprotection and orthogonal amide bond formation. The position of the PBA motif was intended to afford glucose binding on the surface of the assembly. PBAs are capable of forming stable bonds with glucose in water at pH levels at or above their pK_a.[9] Although the pK_a of this amide-linked PBA is around 8.4,[33] the positively charged arginine residues near to the PBA are expected to reduce its pK_a within the range of physiological pH.[34][35]

The expectation when designing PA-PBA was that glucose binding to its PBA motif would stabilize the negatively charged tetrahedral boronate and reduce the net-charge of this otherwise cationic PA to drive nanofiber assembly. However, in its previous use PA-PBA surprisingly formed nanoscale spherical assemblies in the presence of glucose, with these transitioning into liquid–liquid phase-separated droplets upon addition of dasiglucagon.[31] It was therefore hypothesized that PA-PBA did not form the typical high aspect-ratio nanofibers seen for other PAs due to both its relatively short alkyl and β-sheet segments and substantial electrostatic repulsion from its charged and glucose-bound headgroup. With the goal of producing nanofibrillar hydrogels in this work, a diluent PA (dPA, ***Fig 1***) with peptide sequence of C_{10}–$V_2A_2R_3$ was synthesized for co-formulation with PA-PBA to promote intermolecular β-sheet formation and nanofibrillar assembly. The conserved core, β-sheet, and charged regions of the two PAs were intended to facilitate mixing and co-assembly of dPA and PA-PBA.

3.2 Glucose-Dependent Hydrogelation. The goal was to prepare a peptide assembly that was stabilized in the presence of physiologically normal glucose levels, but destabilized under conditions of low glucose to release encapsulated glucagon (***Fig 1***). This follows from other works that used GOx or PBA–glucose binding to enable glucose-stabilized supramolecular peptide assemblies.[29]–[31] The molecular design rationale here was to use dPA to facilitate nanofibrillar assembly and hydrogelation, while PA-PBA imparts glucose-responsiveness to the resulting assemblies through modulating electrostatic interactions as a function of glucose level. Accordingly, different mixing ratios were first explored for glucose-dependent hydrogelation (***Fig S1***). Samples were prepared in HEPES buffer (10 mM, 150 mM NaCl) at a peptide concentration of 2% (w/v) with the addition of either 0 or 100 mg/dL glucose. By itself, PA-PBA formed a clear solution without glucose, becoming a cloudy suspension when glucose was added. This result confirms previous findings that PA-PBA does not gel upon glucose binding.[31] The addition of dPA was next explored to improve β-sheet cohesion and drive nanofiber formation and hydrogelation. PA-PBA and dPA were individually dissolved in 1:1 ACN/H_2O and mixed at a desired mass ratio prior to freeze-drying in order to ensure mixing, with subsequent rehydration under the desired buffer and glucose conditions. Samples were prepared at a total peptide concentration of 2% (w/v) at weight ratios of PA-PBA to dPA of 10%, 20%, 30%, or 40% (***Fig S1***). Samples prepared with 10% or 20% PA-PBA in dPA did not demonstrate any glucose-triggered gelation; though samples became less translucent upon addition of glucose, they did not form self-supporting hydrogels. Interestingly, samples prepared with 30% PA-PBA in dPA exhibited the desired characteristics of a transition from a flowing solution with no glucose to a stable and self-supporting hydrogel at 100 mg/dL glucose. When the ratio was further increased to 40% PA-PBA in dPA, samples formed self-supporting hydrogels with or without glucose. Supposing that the pK_a of the boronate is within the physiologically relevant range, this result implies that some extent of charged boronic acid contributes to reducing the electrostatic repulsion among the headgroups in the mixed PA system to facilitate gelation when present at a high relative amount in the mixture, even in the absence of glucose. Accordingly, the PA-PBA/dPA mixture consisting of 30% PA-PBA was used for all subsequent studies as it displayed the desired gelation properties in this initial screen.

To assess molecular-scale mixing and co-assembly of PA-PBA and dPA in these 30% mixtures, a FAM-modified PA-PBA variant (***Fig S2A***) was synthesized. The extent of self-quenching interactions were then studied, as previously explored,[36] with and without dPA included. FAM-labeled PA-PBA was prepared at a 30% mass ratio in mixture with dPA and compared to FAM-labeled PA-PBA alone at the same total concentration as found in the mixture (***Fig S2B***). The mixed samples exhibited higher fluorescence emission intensity compared to the FAM-labeled PA-PBA alone at the same concentration. As FAM molecules self-quench when in close proximity,[37] this result suggests increased spacing of the FAM fluorophore upon mixture with dPA. While not a direct indication of a homogenous co-assembly, this result nevertheless points to molecular-scale dilution of PA-PBA within dPA, evident by a reduction of self-interactions of the FAM dye, and supports a lack of molecular self-sorting of the peptides in the mixture.

The properties of hydrogels formed by mixing 30% PA-PBA in dPA were further evaluated over a more detailed and broader range of glucose concentrations, from 0 to 200 mg/dL (***Fig 2A***). Self-supporting hydrogels were observed in samples prepared at 50, 100, and 200 mg/dL glucose. The sample prepared with 25 mg/dL glucose formed a very viscous material that flowed slowly following vial inversion,

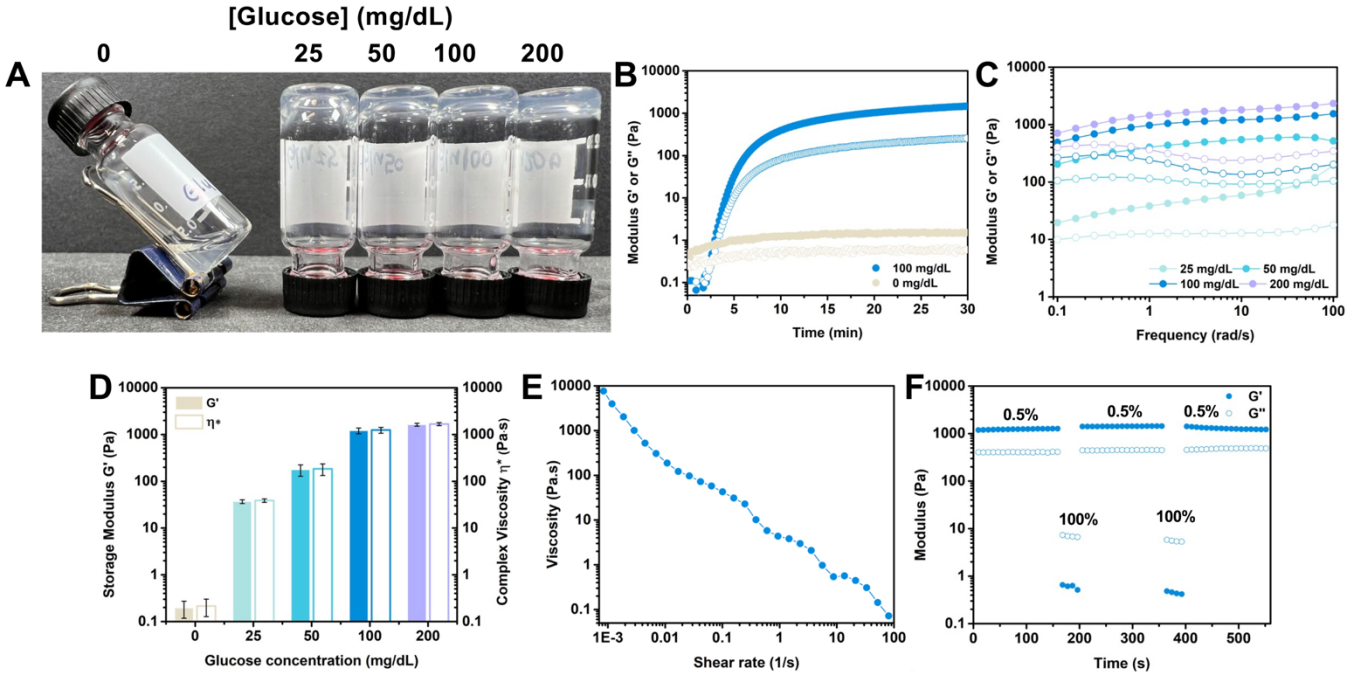

Figure 2. (A) Hydrogelation of co-formulated 30% PA-PBA/dPA mixtures (2% w/v) assessed by vial inversion. **(B)** Evaluation of the storage modulus (G', solid) and loss modulus (G'', open) over time (0.5% strain, 1 rad/s) upon addition of no glucose of 100 mg/dL glucose. **(C)** Rheological frequency sweep (at 0.5% strain) of co-formulated 30% PA-PA/dPA mixtures (2% w/v), where closed symbols are G' and open symbols are G''. **(D)** Storage modulus (*G', solid, left axis*) and complex viscosity (*η*, open, right axis*) following equilibration of hydrogels (2% w/v) over time at 0.5% strain and 1 rad/s; n=2/sample with error bars denoting the experimental range of the two values collected. **(E)** Shear viscosity flow ramp for 30% PA-PA/dPA hydrogel (2% w/v) at 100 mg/dL glucose to demonstrate shear-thinning. **(F)** Step-strain cycling between 0.5% and 100% strain for a 30% PA-PA/dPA hydrogel (2% w/v) at 100 mg/dL glucose.

while the sample prepared with 0 mg/dL glucose again formed a clear solution. To further quantify rheological properties of the 30% PA-PBA/dPA hydrogels upon addition of glucose, a rheological time-course study was next performed (***Fig 2B***). Samples were prepared as described above in either 0 or 100 mg/dL glucose and immediately placed onto the rheometer stage. The storage modulus (G') and loss modulus (G'') were then monitored over the course of 30 min. Both samples began with moduli near to the limit of instrument sensitivity (~1 Pa). However, over the course of the next 10 min, the sample prepared with 100 mg/dL showed a rapid increase in both G' and G'' to approximately 1000 Pa and 100 Pa, respectively. At the endpoint of analysis, plateau values of G' and G'' were measured at 1400 Pa and 200 Pa, respectively. Conversely, the sample prepared without the addition of glucose showed a limited increase in both G' (1.5 Pa) and G'' (0.6 Pa) over the course of evaluation. Though surpassing the rheological threshold for hydrogelation (G'>G''), these values are near to the lower limits of instrument sensitivity and thus are not a reliable indicator of gel formation. Regardless, these data point to significant stabilization and hydrogel stiffening of 3 orders of magnitude upon introduction of a physiologically relevant level of glucose.

To further probe the effects of glucose concentration on mechanical properties of PA-PBA/dPA hydrogels, a frequency sweep was performed on gels prepared in various glucose concentrations of 25, 50, 100, and 200 mg/dL (***Fig 2C***). In spite of their supramolecular and dynamic character, there was limited frequency-dependent behavior observed for these hydrogels over the frequency range evaluated, as G' was in excess of the G'' for the entire range. This feature suggests very slow dynamics and slow stress relaxation for these non-covalent and entangled nanofiber networks.[38] Comparing G' as a function of glucose level revealed trends of increasing hydrogel stiffness as glucose level increased (***Fig 2D***). Samples without glucose were at the lower limits of instrument sensitivity (<1 Pa), while the addition of even a low level of glucose (25 mg/dL) resulted in a G' value of about 40 Pa, further increasing to 180 Pa at 50 mg/dL; these constitute fairly weak hydrogel networks at glucose levels within the physiological range of hypoglycemia. However, at a normal glucose level of 100 mg/dL, hydrogels stiffened to 1200 Pa, with the trend of increasing stiffness continuing to a value of 1800 Pa for moderately high glucose levels of 200 mg/dL. As another measure of glucose-induced change in these materials, the complex viscosity (η*) provides a measure of the total resistance to flow as a function of angular frequency (***Fig 2D***). These values showed a similar trend to those for G', with η* increasing dramatically to 40 Pa·s as glucose levels were increased from 0 to 25 mg/dL. The η* values continued to increase to 200 Pa·s at 50 mg/dL, 1400 Pa·s at 100 mg/dL, and 1900 Pa·s at 200 mg/dL. Accordingly, the addition of glucose drives hydrogelation

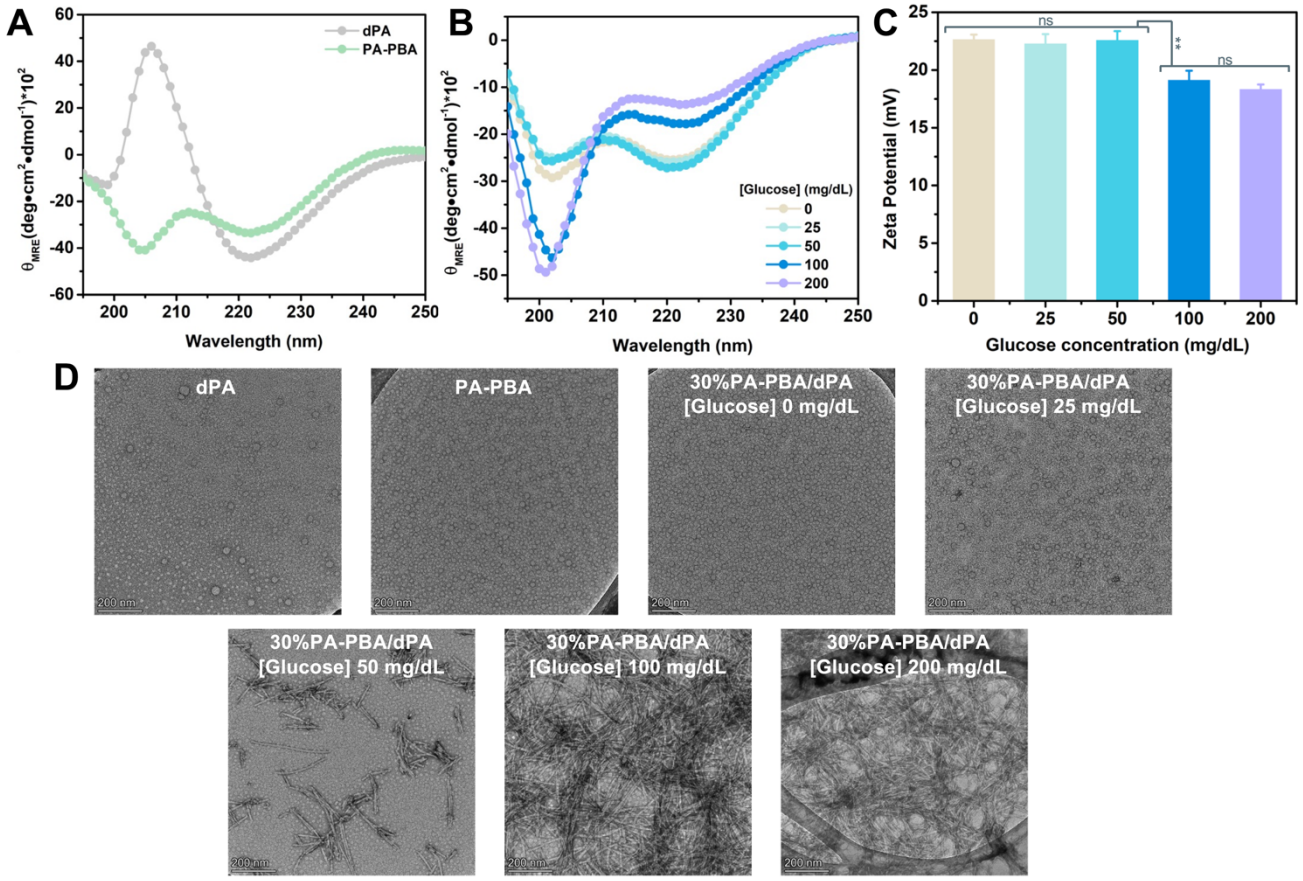

Figure 3. (A) Circular dichroism (CD) spectroscopy of dPA and PA-PBA at 0.5% (w/v). **(B)** CD spectroscopy of co-formulated 30%PA-PBA/dPA mixtures at 0.5% (w/v) with increasing concentration of glucose. **(C)** Zeta potential measurements for 30%PA-PBA/dPA mixtures with increasing concentration of glucose; n=3/sample with error bars denoting standard deviation. A one-way ANOVA with Tukey *post hoc* testing was performed: ns – not significant; ** – P<0.01. **(D)** Transmission electron microscopy (TEM) of dPA, PA-PBA, and 30%PA-PBA/dPA mixtures at various glucose concentrations at 0.1% (w/v).

and increased viscosity in the PA-PBA/dPA mixture, confirming observations from vial inversion.

To probe the potential of these PA-PBA/PA hydrogels to be applied in injection-relevant applications, their ability to shear-thin to pass through a syringe and recover their mechanical properties following the high strain of injection were evaluated. Hydrogels of PA-PBA/dPA prepared at 2% (w/v) and 100 mg/dL glucose were assessed by a shear-ramp experiment (***Fig 2E***), and demonstrated a reduction in viscosity as shear rate increased from an initial "zero-shear" level of 10000 Pa·s to <0.1 Pa·s at 88 s^{-1}. To evaluate their strain recovery, a step-strain experiment was performed by cycling strain between 0.5% and 100% at a frequency of 1 rad/s (***Fig 2F***). With application of high strain, G' was below G''; this indicates disruption of the hydrogel network. However, when returning to a low strain condition, the hydrogel network was immediately recovered (G'>G''). This behavior was maintained for multiple strain cycles with no evidence of deterioration in the structure of the gel network.

3.3 Glucose-Dependent Nanostructure. PA assemblies typically adopt a parallel β-sheet secondary structure with this z-axial hydrogen bonding network underlying high aspect-ratio nanofibrillar assembly.[32] These interactions can be tuned through β-sheet sequence selection to alter the rigidity of the resulting nanofibrillar hydrogels.[39] To assess the impact of molecular design and PA mixing on secondary structure in the PA-PBA/dPA system, CD spectroscopy was performed (***Fig 3A***). By this analysis, dPA had a negative peak at 222 nm and a positive peak at 206 nm; this red-shifted signature is generally indicative of a twisted β-sheet secondary structure. However, PA-PBA exhibited pronounced negative peaks at both 222 nm and 204 nm. Though the additional minima at 204 nm is not a characteristic feature of classical β-sheet structures, it has been reported that this signature can arise from aromatic or distorted β-sheet effects in self-assembling peptides.[40] Here, the aromatic PBA group may impart a similar distorting effect as the native phenylalanine residues used in this prior work. The effect of mixing and addition of glucose was next evaluated for the PA-PBA/dPA mixture prepared at a mass ratio of 30% PA-PBA (***Fig 3B***). The spectra for the co-formulated PA-PBA/dPA mixture in the absence of glucose, as well as under low glucose conditions of 25 and 50 mg/dL, was similar to PA-PBA sample alone with

minima at 222 nm and 203 nm. As glucose was increased to 100 mg/dL, a dramatic shift in the profile of these two minima was observed, with the 203 nm signal becoming more prominent while the intensity of the 222 nm signal decreased. The spectra at 200 mg/dL was generally comparable, though showed additional shifting in the intensity of these two peaks along with a blue-shift of its signal to 201 nm. PBA–glucose binding thus appears to contribute to further distorting the β-sheet structure of the co-formulated PA-PBA/dPA mixtures.

The design of this system envisioned PBA–glucose binding to stabilize the charged tetrahedral boronate species and reduce the magnitude of positive charge in the co-formulated PA-PBA/dPA assemblies. This effect was previously observed for PA-PBA alone, where a steady reduction in positive zeta potential was observed as glucose level increased.[31] Zeta potential measurements were also recorded here for the co-formulated PA-PBA/dPA mixture with glucose varied from 0 to 200 mg/dL (***Fig 3C***). In the absence of glucose, PA-PBA/dPA had a positive zeta potential of 22.5 mV, which showed limited change upon addition of either 25 or 50 mg/dL glucose. A reduction in zeta potential was observed when glucose concentration was increased to 100 mg/dL, measuring 18 mV; increasing glucose to 200 mg/dL offered a slight reduction from this level. These results align with observations from CD, with the increase in glucose from 50 to 100 mg/dL resulting in a clear structural and electrostatic transition in the assemblies.

Samples of each PA alone as well as the co-formulated PA-PBA/dPA mixture at different glucose levels were next investigated for their nanostructure by TEM (***Fig 3D***). All samples were imaged at 0.1% (w/v). In the sample of dPA alone, heterogeneous populations of spherical particles with sizes of 10-40 nm were observed. In the sample of PA-PBA alone, homogeneous spherical assemblies with a diameter of approximately 10 nm were observed; this confirmed a prior report on PA-PBA that showed a preference for nano-spherical rather than traditional nanofibrillar assembly.[31] In the absence of glucose, the co-formulated PA-PBA/dPA mixture also formed spherical nanoparticles of about 10 nm diameter. This nanostructure had no detectable change upon addition of 25 mg/dL glucose. However, when glucose concentration was increased to 50 mg/dL, short fibrillar nanostructures began to appear alongside the spherical nanostructures. Further increasing glucose concentration to 100 or 200 mg/dL led to elongated and entangled nanofiber structures. The emergence of longer nanofibers upon addition of glucose is thus correlated with the glucose-triggered hydrogelation of this material, supporting a mechanism of nanofiber elongation and entanglement leading to hydrogel formation upon PBA–glucose binding. Of note, samples prepared at 0.5% (w/v) and imaged by TEM showed some difference in nanostructure, with very short fibrillar structures observed for both dPA and PA-PBA alone (***Fig S3***). For the PA-PBA/dPA mixture, as glucose increased the nanostructures again demonstrated glucose-dependent nanofiber elongation and entanglement.

3.4 Glucose-Responsive Glucagon Delivery. The performance of co-formulated PA-PBA/dPA hydrogels in the glucose-responsive therapeutic delivery of glucagon was further evaluated. Similar to prior reports,[29]–[31] the objective here was to use these glucose-stabilized materials for glucose-directed delivery of the glucagon hormone that offers a corrective measure for treating low blood glucose. The dasiglucagon analog, which was recently approved by the FDA, is a stabilized modified glucagon used to treat severe hypoglycemia by stimulating the depolymerization and release of stored glycogen to correct blood glucose levels.[41] For ease in quantifying encapsulation and release from co-formulated PA-PBA/dPA hydrogels, a fluorescent methoxycoumarin-4-acetic acid (MCA) conjugated dasiglucagon was synthesized according to prior methods (***Fig S4***).[29] The PA-PBA/dPA hydrogels were mixed with MCA-dasiglucagon in HEPES buffer at physiological glucose levels of 100 mg/dL. These hydrogels were then placed in wells with a bulk buffer of varying glucose level and MCA fluorescence intensity was monitored over time in the bulk phase to quantify release (***Fig 4A***). In the absence of glucose, hydrogels showed very fast drug release, as 54% of MCA-dasiglucagon was released after 5 h incubation. With the addition of low levels of glucose, 25 and 50 mg/dL, the total release amount decreased to 45% and 35% at 5 h, respectively. Further increase in glucose level to a normal level of 100 mg/dL or a hyperglycemic level of 200 mg/dL resulted in 25% and 22% of encapsulated dasiglucagon released, respectively. Taken together with material characterization data, the stabilization of these materials in the presence of glucose facilitated by PBA–glucose binding, enables their use in the responsive delivery of a dasiglucagon therapeutic that itself is a corrective agent for low blood glucose conditions.

Glucose-responsive dasiglucagon delivery from PA-PBA/dPA hydrogels was further validated in a previously established streptozotocin (STZ)-induced type 1 diabetic mouse model recreating hypoglycemia brought about by an insulin overdose (***Fig 4B***).[29] A detailed description of this model using fasted STZ mice to simulate the scenario of protection against a future hypoglycemic episode has been reported elsewhere.[29] In brief, diabetic mice were brought to a normoglycemic level using basal *Insulin Detemir* and then prophylactic function of glucagon-delivery materials was assessed by administration two hours before hypoglycemia was induced by insulin overdose. Blood glucose was collected serially every 30 min throughout the study, with frequency increased to 15 min in the period immediately following insulin overdose. Fasted diabetic mice were corrected to normoglycemia (180-200 mg/dL for mice) by administration of *Insulin Detemir*; after 4 h, 100 μL PA-PBA/dPA hydrogels containing 5 μg dasiglucagon were injected subcutaneously and compared to a control of 5 μg dasiglucagon. Blood glucose levels were monitored throughout the study (***Fig 4C***). Previous studies have shown no therapeutic effect in this model from the administration of "blank" samples of buffer or peptide-based delivery materials alone, with severe hypoglycemia and mortality observed in these groups.[29]–[31] Accordingly, the dasiglucagon delivery function of PA-PBA/dPA hydrogels

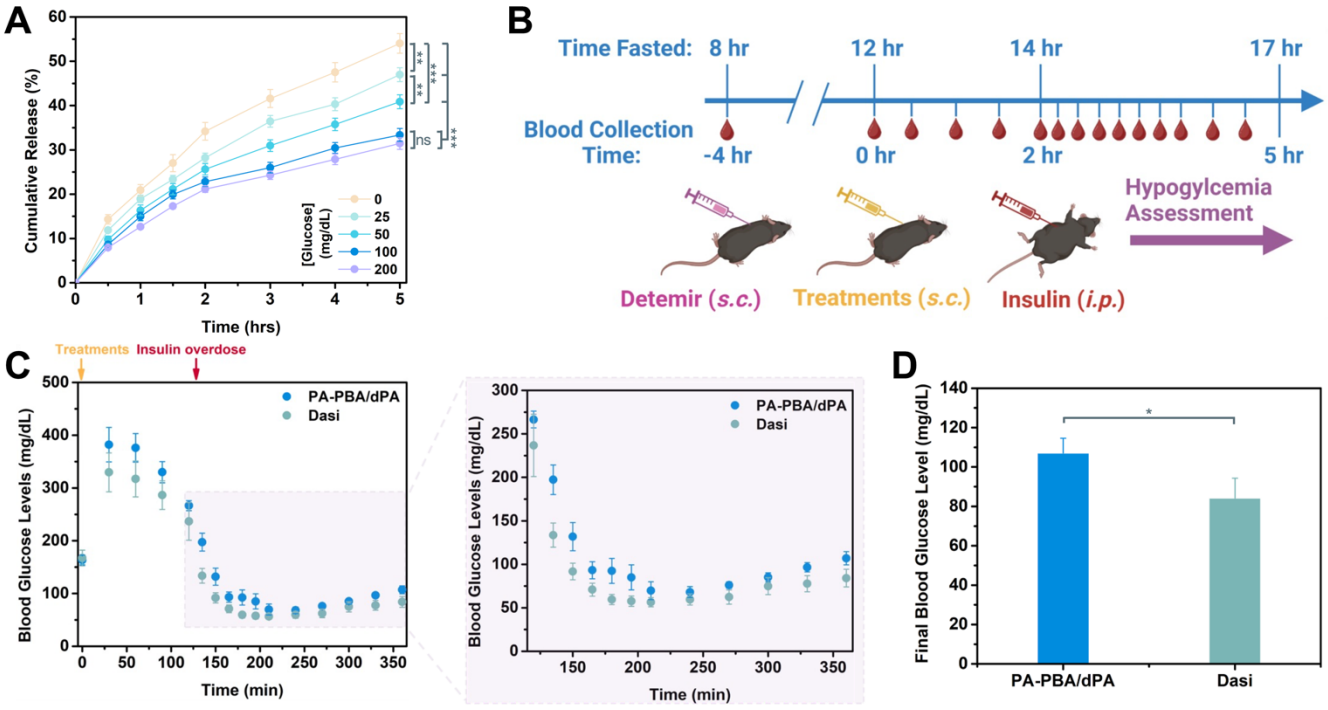

Figure 4. (A) Release profile of encapsulated MCA-dasiglucagon from 30%PA-PBA/dPA hydrogels (2% w/v) prepared in 100 mg/dL glucose and incubated in a bulk buffer containing various glucose concentrations; n=3/ group with mean ± standard deviation shown. A one-way ANOVA with Tukey *post hoc* testing was performed: ns – not significant; ** – P<0.01; *** – P<0.001 **(B)** A mouse model for prophylactic glucagon delivery prior to severe hypoglycemia caused by insulin overdose. **(C)** Blood glucose levels monitored throughout the study, focusing on the region following insulin overdose (gray highlighted panel) and **(D)** final blood glucose levels at the end of study. n=9 mice/group, mean ± SEM shown. *- P < 0.05 by at Student's t-test.

.

was studied in comparison to delivery of the same dose of the agent alone. Mice treated with both the PA-PBA/dPA hydrogel and free dasiglucagon exhibited a dramatic increase in blood glucose following administration; though expected for the free drug, this increase following administration of the hydrogel indicates burst release of some fraction of the therapeutic following injection. This result is consistent with past findings for other glucose-stabilized materials,[29]–[31] pointing to one drawback of using glucose-stabilized hydrogels in this role. Burst release is likewise consistent with the release behavior seen *in vitro* showing some early release into the bulk phase (***Fig 4A***). After 2 h, severe hypoglycemia was induced by intraperitoneal injection of insulin. The hypoglycemic onset was then assessed over 4 h following this insulin overdose (***Fig 4C, inset***). When comparing final blood glucose levels (***Fig 4D***), mice treated with the PA-PBA/dPA hydrogel had significantly higher glucose levels (111 mg/dL) than the free dasiglucagon control (84 mg/dL). This finding suggests some protective function of the PA-PBA/dPA hydrogel in facilitating recovery following hypoglycemia. As another measure of protection, no mortality was observed in the group treated with the PA-PBA/dPA hydrogel, while one animal did not survive in the control group. The performance of the PA-PBA/dPA hydrogel was generally consistent with the results of other glucose-stabilized materials in this same animal model.[29]–[31] As was the case in these other platforms, leakage of dasiglucagon following administration remains an issue, manifest in elevated blood glucose levels upon injection and prior to insulin overdose. The improvements in hypoglycemic outcomes suggests PA-PBA/dPA hydrogels offer similar protection as these previous platforms via more controlled and glucose-directed release mechanisms, yet further work is necessary to validate glucose-responsive release of glucagon from these material depots in response to hypoglycemia, such as by quantification of serum dasiglucagon levels over time. Accordingly, the current study lends further support to the concept of using glucose-stabilized materials to provide preventative support in advance of a hypoglycemic episode, yet does not address the repeated issue of dasiglucagon leakage following administration that remains a drawback of this approach that would confound insulin-centered blood glucose control in treating type 1 diabetes.

Conclusions

This work successfully demonstrates the development of a glucose-responsive supramolecular PA-PBA hydrogel system for glucagon delivery. The design strategy exploits glucose as a molecular trigger to drive nanofiber assembly and gelation at physiological glucose levels, which then disassembles under hypoglycemic conditions to release the encapsulated therapeutic. The tunable nature of the assembly, characterized by changes in electrostatic interactions and nanostructure morphology, provides a means of controlling glucagon release at rates inversely related to glucose level. Studies *in vitro* highlight responsiveness to varying glucose concentrations, while the

in vivo results in a type 1 diabetic mouse model demonstrate the protective effect of the PA-PBA hydrogel in mitigating hypoglycemia. However, while the hydrogel system showed potential for controlled glucagon delivery, the observed burst release following initial injection suggests that further refinement is required to achieve a more sustained release profile. Modifications to reduce the initial burst while maintaining responsiveness to low glucose could further improve the therapeutic efficacy of the system. Future studies should explore alternative formulations and co-delivery strategies to optimize glucagon release under hypoglycemic conditions.

Overall, this study provides valuable insights into the design of glucose-responsive materials and highlights the broader application of supramolecular systems for therapeutic delivery. The ability to modulate drug release in response to environmental cues, such as glucose levels, presents exciting possibilities for precision medicine approaches, especially in the treatment of diabetes. The PA-PBA system offers a platform for further development and could be adapted for other therapeutic delivery applications where responsive, on-demand, glucose-responsive drug release is required.

Acknowledgments

MJW gratefully acknowledges funding support for this work from the Helmsley Charitable Trust (grants 2019PG-T1D016 and 2102-04994), the American Diabetes Association Pathway Accelerator Award (1-19-ACE-31), Breakthrough T1D (5-CDA-2020-947-A-N), and a National Science Foundation CAREER award (BMAT, 1944875). Portions of Figures 1 and 4 prepared using Biorender.com.

Other Information

Supplementary information The online version contains supplementary material available at:

Correspondence and requests for materials should be addressed to Matthew J. Webber, mwebber@nd.edu

References

1. Myers MG Jr, Affinati AH, Richardson N, Schwartz MW. Central nervous system regulation of organismal energy and glucose homeostasis. Nat Metab. 2021;3:737–50.
2. Drucker DJ. The role of gut hormones in glucose homeostasis. J Clin Invest. American Society for Clinical Investigation; 2007;117:24–32.
3. Röder PV, Wu B, Liu Y, Han W. Pancreatic regulation of glucose homeostasis. Exp Mol Med. 2016;48:e219.
4. Holst JJ, Gasbjerg LS, Rosenkilde MM. The role of incretins on insulin function and glucose homeostasis. Endocrinology. 2021;162:bqab065.
5. Badeau BA, DeForest CA. Programming stimuli-responsive behavior into biomaterials. Annu Rev Biomed Eng. Annual Reviews; 2019;21:241–65.
6. Koetting MC, Peters JT, Steichen SD, Peppas NA. Stimulus-responsive hydrogels: Theory, modern advances, and applications. Mater Sci Eng R Rep. 2015;93:1–49.
7. Walther A. Viewpoint: From Responsive to Adaptive and Interactive Materials and Materials Systems: A Roadmap. Adv Mater. 2020;32:e1905111.
8. Mohanty AR, Ravikumar A, Peppas NA. Recent advances in glucose-responsive insulin delivery systems: novel hydrogels and future applications. Regen Biomater. 2022;9:rbac056.
9. Xiang Y, Su B, Liu D, Webber MJ. Managing diabetes with hydrogel drug delivery. Adv Ther. Wiley; 2024;7:2300127.
10. VandenBerg MA, Webber MJ. Biologically Inspired and Chemically Derived Methods for Glucose-Responsive Insulin Therapy. Adv Healthc Mater. 2019;8:e1801466.
11. Wang J, Wang Z, Yu J, Kahkoska AR, Buse JB, Gu Z. Glucose-Responsive Insulin and Delivery Systems: Innovation and Translation. Adv Mater. 2020;32:e1902004.
12. Cho NH, Shaw JE, Karuranga S, Huang Y, da Rocha Fernandes JD, Ohlrogge AW, Malanda B. IDF Diabetes Atlas: Global estimates of diabetes prevalence for 2017 and projections for 2045. Diabetes Res Clin Pract. 2018;138:271–81.
13. Webber MJ, Appel EA, Meijer EW, Langer R. Supramolecular biomaterials. Nat Mater. 2016;15:13–26.
14. Webber MJ, Langer R. Drug delivery by supramolecular design. Chem Soc Rev. 2017;46:6600–20.
15. Sahoo JK, VandenBerg MA, Webber MJ. Injectable network biomaterials via molecular or colloidal self-assembly. Adv Drug Deliv Rev. 2018;127:185–207.
16. Mart RJ, Osborne RD, Stevens MM, Ulijn RV. Peptide-based stimuli-responsive biomaterials. Soft Matter. 2006;2:822–35.
17. Webber MJ. Engineering responsive supramolecular biomaterials: Toward smart therapeutics. Bioeng Transl Med. 2016;1:252–66.
18. Webber MJ, Pashuck ET. (Macro)molecular self-assembly for hydrogel drug delivery. Adv Drug Deliv Rev. 2021;172:275–95.
19. Matson JB, Zha RH, Stupp SI. Peptide Self-Assembly for Crafting Functional Biological Materials. Curr Opin Solid State Mater Sci. 2011;15:225–35.
20. Zhang S. Fabrication of novel biomaterials through molecular self-assembly. Nat Biotechnol. 2003;21:1171–8.
21. Li Y, Wang F, Cui H. Peptide-based supramolecular hydrogels for delivery of biologics. Bioeng Transl Med. 2016;1:306–22.
22. Levin A, Hakala TA, Schnaider L, Bernardes GJL, Gazit E, Knowles TPJ. Biomimetic peptide self-assembly for functional materials. Nat Rev Chem. 2020;4:615–34.
23. Yu S, Webber MJ. Engineering disease analyte response in peptide self-assembly. J Mater Chem B. 2024;12:10757–69.
24. Li Z, Zhu Y, Matson JB. pH-Responsive Self-Assembling Peptide-Based Biomaterials: Designs and Applications. ACS Appl Bio Mater. 2022;5:4635–51.
25. Zelzer M, Todd SJ, Hirst AR, McDonald TO, Ulijn RV. Enzyme responsive materials: design strategies and future developments. Biomater Sci. 2013;1:11–39.
26. Jin H, Sun M, Shi L, Zhu X, Huang W, Yan D. Reduction-responsive amphiphilic polymeric prodrugs of camptothecin-polyphosphoester for cancer chemotherapy. Biomater Sci. 2018;6:1403–13.
27. Fu M, Zhang C, Dai Y, Li X, Pan M, Huang W, Qian H, Ge L. Injectable self-assembled peptide hydrogels for glucose-mediated insulin delivery. Biomater Sci. 2018;6:1480–91.
28. Li X, Fu M, Wu J, Zhang C, Deng X, Dhinakar A, Huang W, Qian H, Ge L. pH-sensitive peptide hydrogel for glucose-responsive insulin delivery. Acta Biomater. 2017;51:294–303.
29. Yu S, Xian S, Ye Z, Pramudya I, Webber MJ. Glucose-Fueled Peptide Assembly: Glucagon Delivery via Enzymatic

Actuation. J Am Chem Soc. 2021;143:12578–89.

30. Yu S, Ye Z, Roy R, Sonani RR, Pramudya I, Xian S, Xiang Y, Liu G, Flores B, Nativ-Roth E, Bitton R, Egelman EH, Webber MJ. Glucose-triggered gelation of supramolecular peptide nanocoils with glucose-binding motifs. Adv Mater. 2024;36:2311498.
31. Yu S, Chen W, Liu G, Flores B, DeWolf EL, Fan B, Xiang Y, Webber MJ. Glucose-Driven Droplet Formation in Complexes of a Supramolecular Peptide and Therapeutic Protein. J Am Chem Soc. 2024;146:7498–505.
32. Cui H, Webber MJ, Stupp SI. Self-assembly of peptide amphiphiles: from molecules to nanostructures to biomaterials. Biopolymers. 2010;94:1–18.
33. Marco-Dufort B, Tibbitt MW. Design of moldable hydrogels for biomedical applications using dynamic covalent boronic esters. Mater Today Chem. Elsevier BV; 2019;12:16–33.
34. Kitano S, Hisamitsu I, Koyama Y, Kataoka K, Okano T, Sakurai Y. Effect of the incorporation of amino groups in a glucose-responsive polymer complex having phenylboronic acid moieties. Polym Adv Technol. Wiley; 1991;2:261–4.
35. Shiino D, Kubo A, Murata Y, Koyama Y, Kataoka K, Kikuchi A, Sakurai Y, Okano T. Amine effect on phenylboronic acid complex with glucose under physiological pH in aqueous solution. J Biomater Sci Polym Ed. 1996;7:697–705.
36. Chen W, Xian S, Webber B, DeWolf EL, Schmidt CR, Kilmer R, Liu D, Power EM, Webber MJ. Engineering supramolecular nanofiber depots from a glucagon-like peptide-1 therapeutic. ACS Nano. 2024;18:31274–85.
37. Ren C, Wang H, Mao D, Zhang X, Fengzhao Q, Shi Y, Ding D, Kong D, Wang L, Yang Z. When molecular probes meet self-assembly: an enhanced quenching effect. Angew Chem Int Ed Engl. 2015;54:4823–7.
38. Webber MJ, Tibbitt MW. Dynamic and reconfigurable materials from reversible network interactions. Nature Reviews Materials. 2022;7:541–56.
39. Pashuck ET, Cui H, Stupp SI. Tuning supramolecular rigidity of peptide fibers through molecular structure. J Am Chem Soc. 2010;132:6041–6.
40. Lee NR, Bowerman CJ, Nilsson BL. Effects of varied sequence pattern on the self-assembly of amphipathic peptides. Biomacromolecules. 2013;14:3267–77.
41. Blair HA. Dasiglucagon: First Approval. Drugs. 2021;81:1115–20.